Available online at www.sciencedirect.com
SCIENCE DIRECT®
International Journal of Heat and Fluid Flow 25 (2004) 683–691
International Journal of HEAT AND FLUID FLOW
www.elsevier.com/locate/ijhff

Effect of natural convection on laser chemical vapor deposition with a stationary laser beam

Yuwen Zhang *

Department of Mechanical and Aerospace Engineering, University of Missouri—Columbia, E2412 Engineering Building East, Columbia, MO 65211, USA

Received 20 October 2003; accepted 8 January 2004
Available online 26 February 2004

Abstract

Effect of natural convection on laser chemical vapor deposition (LCVD) of titanium nitride on a finite slab under irradiation by a stationary laser beam is investigated numerically. Natural convection due to temperature and concentration differences in the gases mixture is modeled and implemented into the thermal model of LCVD. The results show that the effect of natural convection on the shape of deposited film is very insignificant for all cases studied. The effects of laser beam properties and initial pressure of the source gases are also investigated.

Keywords: Heat transfer; Laser; Mass transfer; Natural convection; Vapor deposition

1. Introduction

Selective area laser deposition (SALD) is an emerging manufacturing technology that directly creates three-dimensional parts from a CAD design (Conley and Marcus, 1997). It utilizes laser chemical vapor deposition (LCVD) technique, which can be based on reactions initiated pyrolytically, photolytically or a combination of both (Marcus et al., 1993), to deposit the film at the desired location on the substrate. LCVD can also find its application on thin film coating and semiconductor applications.

Chemical vapor deposition (CVD) has been extensively investigated by many researchers. The distinctive feature of LCVD, compared with the regular CVD, is that only a very small spot on the substrate is heated by the laser beam and vapor deposition occurs only on the heated spot. A very detailed literature review about laser chemical vapor deposition (LCVD) was given by Mazumder and Kar (1995). Marcus et al. (1993) studied the residual stresses in laser processed solid freeform fabrication (SFF), which includes SALD. Heat conduction in the substrate is modeled as a pure conduction problem with a moving heat source. Jacquot et al. (1995) proposed a thermal model of the SALD process using acetylene (C_2H_2) as the source gas. Various phenomena, which include heat conduction in the substrate, chemical reaction during carbon deposit, and mass diffusion of acetylene in the chamber are taken into account. The effect of chemical reaction heat on the heat conduction of the substrate was also taken into account. The temperature of the gases was assumed to be uniform and therefore the heat transfer in the gas phase is neglected. Zhang and Fgahri (2000) developed a very detailed thermal model of SALD process, which includes the submodels of heat transfer, chemical reaction and mass transfer, and the model was employed to simulate the laser chemical vapor deposition of TiN film on a finite slab with stationary and moving laser beams. The results showed that the effect of chemical reaction heat on the shape of deposited film was negligible. Zhang (2003a) performed a parametric study on shape and cross-sectional area of the thin film produced by LCVD with a moving laser beam. The effects of laser scanning velocity, laser power and radius of the laser beam on the shapes of the deposited film were investigated and an empirical correlation was obtained.

The spot on the substrate under laser irradiation is at a very high temperature. The temperature difference in

* Tel.: +1-573-882-2785; fax: +1-573-884-5090.

0142-727X/$ - see front matter © 2004 Elsevier Inc. All rights reserved.
doi:10.1016/j.ijheatfluidflow.2004.01.001

Nomenclature

A	half-length of the chamber (m)
a	half-length of the substrate (m)
B	half-width of the chamber (m)
b	half-width of the substrate (m)
C	concentration (kg/m^3)
c_p	specific heat (J/kg K)
D	mass diffussivity (m^2/s)
E	activation energy (kJ/mol)
H	height of the chamber (m)
h	thickness of the substrate (m)
k	thermal conductivity (W/m K)
K_0'	Arrhenius constant
M	molecular weight (g/mol)
m	mass flux (kg/m^2)
P	laser power (W)
p	pressure (Pa)
q''	heat flux (W/m^2)
r_0	radius of the laser beam (m)
R_u	universal gas constant ($=8.314$ kJ/kmol)
S	source term in the energy equation
S_c	source term in the mass transfer equation
t	time (s)
T	temperature (K)
u	velocity component in x direction (m/s)
v	velocity component in y direction (m/s)
w	velocity component in z direction (m/s)
x	coordinate in length direction (m)
y	coordinate in width direction (m)
z	coordinate height direction (m)

Greeks

α_a	absorptivity
β	coefficients of thermal expansion
β_c	concentration expansion coefficients
γ	sticking coefficient
δ	thickness of the deposited film (m)
ΔH_R	heat of chemical reaction (J/kg)
ε	emissivity
ρ	density (kg/m^3)

Subscripts

g	gas
i	initial value
s	substrate
∞	infinite

the source gases will cause natural convection in the chamber. The concentration of the gas mixture near the hot spot on the substrate is affected by the chemical reaction that takes place on the substrate. The concentration difference in the chamber becomes another driving force of natural convection in the chamber. The effect of natural convection due to temperature and concentration differences in the gases is neglected by most researchers (Jacquot et al., 1995; Kar et al., 1991; Conde et al., 1992). Lee et al. (1995) numerically predicted the deposit rate using pure tetramethylsilane [$Si(CH_3)_4$] as a precursor for a rod grown by the SALD process. They concluded that the heat and mass transfer in the gases were dominated by diffusion, and the effect of natural convection of the gas on the thin film deposition rate was negligible. Zhang (2003b) investigated the quasi-steady state natural convection in LCVD process with moving laser beam. The problem is formulated in the coordinate system that moves with the laser beam and therefore, the problem is a quasi-steady state problem. The results show that the effect of natural convection on the shape of deposited film is negligible for the laser power of $P = 300$ W. When the laser power is increased to 360 W, the effect of natural convection on the shape of the cross section becomes important although the cross sectional area is almost unchanged. A groove is observed on the top of the deposited film for $P = 360$ W due to low sticking coefficient.

LCVD can also find its application in micromanufacturing such as deposition of rods, fibers, coils (Duty et al., 2001). Maxwell et al. (1998a) successfully fabricated high field density microsolenoids from 100 to 500 μm in diameter using 3-D LCVD technique. Maxwell et al. (1999) and Williams et al. (1999) deposited carbon in the form of helical spring and the fiber diameter of the spring was as small as 5 μm and the spring inner diameter was as small as 60 μm. Maxwell et al. (1998b) deposited high-aspect-ratio titanium nitride needles up to 12 mm long using $Ti[N(CH_3)_2]_4$ as precursor. During growth of rods and fibers, the laser beam is usually stationary. In order to reveal the role of natural convection during micromanufacturing process, the effect of natural convection on the temperature distribution and the shape of the deposited film in a LCVD process with stationary laser beam will be investigated.

2. Physical model

The physical model of LCVD is illustrated in Fig. 1. A substrate made of Incoloy 800 with a size of $2a \times 2b \times h$ (length × width × height) is located in the center of the bottom surface of a chamber with a size of $2A \times 2B \times H$ (length × width × height). Before the vapor deposition started, the chamber is evacuated and then filled with mixture of H_2, N_2, and $TiCl_4$. The center of the laser

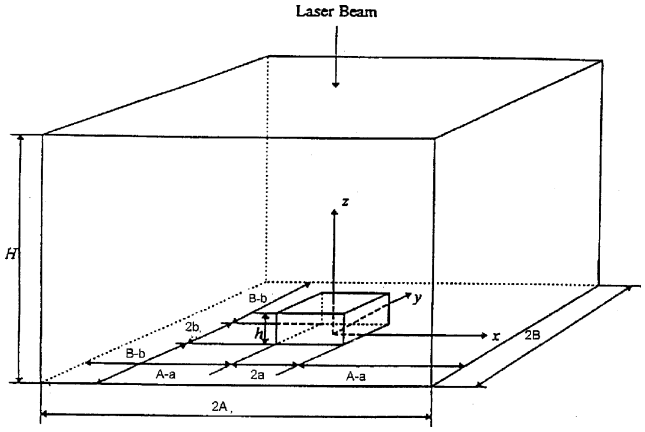

Fig. 1. Physical model of laser chemical vapor deposition.

beam is located at the center of the top surface of the substrate $(x = 0, y = 0, z = h)$. The vapor deposition starts after the surface temperature reaches to the threshold temperature for chemical reaction (1173 K; Conde et al., 1992). The chemical reaction that takes place on the top substrate surface absorbs part of the laser energy and consumes the $TiCl_4$ near the substrate surface. A concentration difference is therefore established and becomes the driving force of mass transfer. The physical model of the SALD process will include: natural convection, heat transfer in the substrate and gases, chemical reaction, as well as mass transfer in the gases.

Since the temperature of the substrate undergoes a significant change under laser irradiation, the constant thermal properties assumption does not apply (Jacquot et al., 1995; Lee et al., 1995; Kar and Mazumder, 1989; Zhang and Fgahri, 2000). Heat transfer in the substrate and gases is modeled as one problem with thermal properties reflecting the differences in each region. In the substrate region, the velocity will be set to zero in the numerical solution. The advantage of modeling the conduction problem in the substrate and the gases as one problem is that the temperature distribution in substrate and gases can be obtained by solving one equation, and the iteration procedure to match the boundary condition at substrate–gases interface can therefore be eliminated. Since the problem is symmetric about the xz plane and yz plane, only quarter of the problem need to be investigated. For a coordinate system shown in Fig. 1, the heat transfer in the substrate and gases are modeled with the following equations:

$$\frac{\partial \rho}{\partial t} + \frac{\partial(\rho u)}{\partial x} + \frac{\partial(\rho v)}{\partial y} + \frac{\partial(\rho w)}{\partial z} = 0 \tag{1}$$

$$\frac{\partial u}{\partial t} + u\frac{\partial u}{\partial x} + v\frac{\partial u}{\partial y} + w\frac{\partial u}{\partial z} = -\frac{1}{\rho}\frac{\partial p}{\partial x} + \nu\left(\frac{\partial^2 u}{\partial x^2} + \frac{\partial^2 u}{\partial y^2} + \frac{\partial^2 u}{\partial z^2}\right) \tag{2}$$

$$\frac{\partial v}{\partial t} + u\frac{\partial v}{\partial x} + v\frac{\partial v}{\partial y} + w\frac{\partial v}{\partial z} = -\frac{1}{\rho}\frac{\partial p}{\partial y} + \nu\left(\frac{\partial^2 v}{\partial x^2} + \frac{\partial^2 v}{\partial y^2} + \frac{\partial^2 v}{\partial z^2}\right) \tag{3}$$

$$\frac{\partial w}{\partial t} + u\frac{\partial w}{\partial x} + v\frac{\partial w}{\partial y} + w\frac{\partial w}{\partial z} = -\frac{1}{\rho}\frac{\partial p}{\partial z} + \nu\left(\frac{\partial^2 w}{\partial x^2} + \frac{\partial^2 w}{\partial y^2} + \frac{\partial^2 w}{\partial z^2}\right) - g\beta(T - T_\infty) - g\beta_c(C - C_\infty) \tag{4}$$

$$\rho\left[\frac{\partial(c_p T)}{\partial t} + \frac{\partial(u c_p T)}{\partial x} + \frac{\partial(v c_p T)}{\partial y} + \frac{\partial(w c_p T)}{\partial z}\right] = \frac{\partial}{\partial x}\left(k\frac{\partial T}{\partial x}\right) + \frac{\partial}{\partial y}\left(k\frac{\partial T}{\partial y}\right) + \frac{\partial}{\partial z}\left(k\frac{\partial T}{\partial z}\right) + S \tag{5}$$

$$\frac{\partial C}{\partial t} + \frac{\partial(uC)}{\partial x} + \frac{\partial(vC)}{\partial y} + \frac{\partial(wC)}{\partial z} = D\left(\frac{\partial^2 C}{\partial x^2} + \frac{\partial^2 C}{\partial y^2} + \frac{\partial^2 C}{\partial z^2}\right) + S_c \tag{6}$$

where β and β_c are respectively the coefficients of thermal expansion and concentration expansion coefficient, respectively.

The thermal properties are different for substrate and gases. For the substrate region, the thermal properties is that of the substrate material, Incoloy 800. For the gases region, the thermal properties are determined by the individual thermal properties of H_2, N_2, and $TiCl_4$ as well as their molar fractions (Zhang and Fgahri, 2000). The mass diffusivity of $TiCl_4$ in the gas mixture is determined by Stefan–Maxwell equation (Bird et al., 1960) using the binary diffusivity of $TiCl_4$ with respect to each other species, which is calculated using the hard sphere model.

The source term in Eq. (5) deals with the effect of laser beam heating and chemical reaction. The source term will be zero everywhere except at the substrate–gases interface under the laser spot. The heat flux at the substrate surface due to laser beam irradiation and chemical reaction is expressed as

$$q'' = \frac{2P\alpha_a}{\pi r_0^2}\exp\left[-\frac{2(x^2 + y^2)}{r_0^2}\right] - \varepsilon\sigma(T^4 - T_\infty^4) - \rho_{TiN}\Delta H_R\frac{d\delta}{dt}, \quad z = h \tag{7}$$

where $d\delta/dt$ is the deposit rate. For a chemical reaction in the order of unity, the deposition rate is expressed as (Zhang and Fgahri, 2000)

$$\frac{d\delta}{dt} = \frac{\dot{m}}{\rho_{TiN}} = \frac{\gamma_{TiN}K_0}{\rho_{TiN}}\exp\left(-\frac{E}{R_u T_s}\right)C_s \tag{8}$$

where C_s represents the concentration of $TiCl_4$ at the surface of the substrate. The constant, K_0, in Eq. (8) is defined as

$$K_0 = C_{H_2} C_{N_2}^{1/2} K_0' \tag{8a}$$

where C_{H_2} and C_{N_2} are the concentrations of hydrogen and nitrogen, and K_0' is the Arrhenius constant. Since the concentrations of hydrogen and nitrogen are at least one order of magnitude higher than that of $TiCl_4$, it is assumed that C_{H_2} and C_{N_2} remain unchanged during the deposition process. It is also necessary to point out that Eq. (8) is applicable for growth on a flat substrate, which is the case for initial deposition of the thin film on the substrate investigated in this paper.

In order to use Eq. (7) to determine the source term in Eq. (5), the heat flux is treated as an internal heat source in the grid near the surface of the substrate, i.e.

$$S = \frac{q''\Delta x\Delta y}{\Delta V} = \frac{q''}{\Delta z} \tag{9}$$

where Δx, Δy, Δz represent the dimension of the control volume cell in the substrate near its surface.

The effect of the chemical reaction on the mass transfer is accounted for by a source term in Eq. (6). The mass flux rate of $TiCl_4$ at the substrate is expressed as

$$\dot{m}_{TiCl_4} = \rho_{TiN} \frac{d\delta}{dt} \frac{M_{TiCl_4}}{M_{TiN}}, \quad z = h \tag{10}$$

The source term in Eq. (6) is then expressed as

$$S_c = -\frac{\dot{m}_{TiCl_4}\Delta x\Delta y}{\Delta V} = \frac{M_{TiCl_4}}{M_{TiN}} \frac{K_0}{\Delta z} \exp\left(-\frac{E}{R_u T_s}\right) C_s, \quad z = h \tag{11}$$

The initial and boundary conditions of the velocities are

$$u = v = w = 0, \quad 0 \leqslant x \leqslant A \quad 0 \leqslant y \leqslant B \quad 0 \leqslant z \leqslant H \quad t = 0 \tag{12a}$$

$$u = \frac{\partial v}{\partial x} = \frac{\partial w}{\partial x} = 0, \quad x = 0 \tag{12b}$$

$$u = v = w = 0, \quad x = A \tag{12c}$$

$$v = \frac{\partial u}{\partial y} = \frac{\partial w}{\partial y} = 0, \quad y = 0 \tag{12d}$$

$$u = v = w = 0, \quad y = B \tag{12e}$$

$$u = v = w = 0, \quad z = 0, H \tag{12f}$$

The initial and boundary conditions of Eqs. (5) and (6) are

$$T = T_i, \quad C = C_i, \quad 0 \leqslant x \leqslant A \quad 0 \leqslant y \leqslant B \quad 0 \leqslant z \leqslant H \quad t = 0 \tag{13a}$$

$$\frac{\partial T}{\partial x} = \frac{\partial C}{\partial x} = 0, \quad x = 0, A \tag{13b}$$

$$\frac{\partial T}{\partial y} = \frac{\partial C}{\partial y} = 0, \quad y = 0, B \tag{13c}$$

$$\frac{\partial T}{\partial z} = 0, \quad z = 0, H \tag{13d}$$

$$\frac{\partial C}{\partial z} = 0, \quad z = 0, \quad x > a \;\; y > b \tag{13e}$$

$$C = 0, \quad z = 0, \quad x \leqslant a \;\; y \leqslant b \tag{13f}$$

$$\frac{\partial C}{\partial z} = 0, \quad z = H \tag{13g}$$

3. Numerical solution

The problem under investigation is a conjugated natural convection problem driving by temperature and concentration differences. The governing equations are discretized using the finite volume method (Patankar, 1980). The SIMPLEC algorithm (Van Doormaal and Raithby, 1984) was employed to handle the linkage between velocity and pressure. The staggered grid was used to discretize solution domain. The pressure, temperature, concentration, and all properties are stored on the main grid, which is at the center of the control volume. The velocity components are calculated at the point that lie on the faces of the control volumes. The convection-diffusion terms in the momentum, energy and concentration equations are discretized by a exponential scheme. The resulted discrete equations are solved by using ADI (alternative directional implicit) method. The underrelaxation factor for the velocity components is 0.5. Underrelaxation for pressure is not needed because SIMPLEC algorithm is employed.

The governing equations are written for the entire domain that includes both substrate and the gases. The velocity and concentration in the substrate region should be zero. The algebraic equations resulted from the control volume approach have the following format

$$a_P \phi_P = \sum a_{nb} \phi_{nb} + b \tag{14}$$

By setting $a_P = 10^3$ in Eq. (14) at the grid point located in the substrate region for momentum equations and mass transfer equation, the zero velocity and concentrate field can be achieved (Yang and Tao, 1992). In order to ensure that the velocity field is not altered by the pressure correction, the pressure correction at the points in the substrate region must be zero. The above technique is also applied to achieve the zero pressure correction. The coefficients of the algebraic equations are altered before the algebraic equations are solved.

Natural convection and chemical reaction are coupled and therefore iteration is needed. The overall iteration for a time step is performed for the deposit rate, $d\delta/dt$, and the procedure is outlined as follows:

1. Guess a distribution of deposit rate, $d\delta/dt$.
2. Solve for the velocities, pressure, temperature, and concentration distribution in substrate and gases.
3. Calculate the deposit rate, $(d\delta/dt)_{new}$ from Eq. (8).
4. Compare the deposit rate obtained in step 4 with the guessed distribution in step 1. If $|(d\delta/dt)_{new} - d\delta/dt| \leqslant e$ where e is a small tolerance value, end the iteration and go to the next time step. If not, update the value of $d\delta/dt$ and go back to step 1.

During the above iteration procedure, an underrelaxation with underrelaxation factor of 0.5 is necessary. After grid size and time step test, the calculations were carried out for a non-uniform grid of 42 nodes in the x and y direction and 82 nodes in the z direction with a time step of 0.005 s.

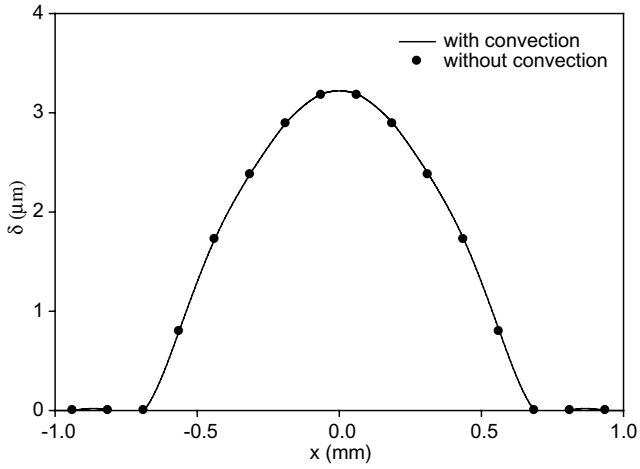

Fig. 2. Effect of convection on the deposited film thickness ($P = 300$ W, $t = 2$ s).

4. Results and discussion

The geometric and physical parameters are similar to those in Zhang and Fgahri (2000). The size of the chamber is $2A \times 2B \times H = 0.5 \times 0.5 \times 0.125$ m^3, and the substrate is $2a \times 2b \times h = 0.01 \times 0.01 \times 0.005$ m^3. The radius of the laser beam, which is defined as the radius where the laser intensity is $1/e^2$ of the intensity at the center of the laser beam, is 1.0×10^{-3} m to 1.5×10^{-3} m. The absorptivity of the laser beam at the substrate surface is taken to be 0.23 (Conde et al., 1992). The activation energy of the chemical reaction is taken to be $E = 51.02$ kJ/mol (Conde et al., 1992). The constant K_0, as defined in Eq. (12a), is 8.4 m/s. Chemical reaction heat, ΔH_R, as determined using JANAF thermochemical tables (Chase, 1986), is 5.379×10^5 J/kg.

Fig. 2 shows the variation of deposited TiN film thickness with different x but $y = 0$. The deposited film thickness obtained by models with and without convection are plotted. The total pressure in the chamber is 207 Torr and the partial pressure of titanium chloride is maintained at 7 Torr. The partial pressures of N_2 and H_2 are the same. The power of the laser beam and the irradiate time are respectively 300 W and 2 s. It can be seen that the deposited TiN film thicknesses obtained by models with and without convection are very close: the difference at the center of the laser beam is only 0.025%. Fig. 3 shows the velocity component in z direction at the end of the process $(t = 2)$ s. Since chemical reaction takes place on the hot spot of substrate under laser irradiation, gases flow toward the hot spot due to consumption of $TiCl_4$. Therefore, the velocity component in z direction is negative at $z = 0.00522$ m, which is only 0.22 mm above the top of the substrate surface. At another height, $z = 0.0081$ m, the velocity component in z direction near the center of the laser beam is positive due to natural convection driven by the temperature gradient in the gases. Fig. 4 illustrates a temperature contour at $y = 0$ surface at the end of the process ($t = 2$ s). The isothermal line for $T = 750$ and 1100 K for the cases with and without convection are almost the same, which explains the reason that the deposited TiN film thickness profile is almost not affected by convection. On the other hand, the isothermal lines for $T = 400$ K are significantly different for cases with and without convection.

Fig. 5 shows predicted deposited TiN film thickness with the power of the laser beam and the irradiate time of 400 W and 2 s. Volcano-like profiles of deposited film were often reported for the LCVD process (Lee et al., 1995) and the causes were not clear. Conde et al. (1992) suggested that the low sticking coefficient at the center of the laser beam, where the temperature is highest, plays a major role. In order to predict volcano-like deposited film, a sticking coefficient, γ_{TiN}, introduced by Conde et al. (1992) is employed. It can be seen that the volcano-like deposited film shape is successfully predicted by using the temperature dependence of the sticking coefficient introduced by Conde et al. (1992). Similar to the case with laser power of 300 W and irradiation time of 2 s, the effect of convection on the deposited film thickness is very insignificant. Fig. 6 shows the velocity components in z direction at the end of the process $(t = 2)$ s. Fig. 6(a) indicates that the absolute value of the maximum velocity in z direction at the center of the laser beam is more than doubled compared to the case with a laser power of 300 W. The effect of laser power on the profile of the velocity component in z direction at $z = 0.0081$ m is not very significant. Fig. 7 illustrates a temperature contour at $y = 0$ surface at the end of the process ($t = 2$ s). The isothermal lines for $T = 400$ K are significantly distorted due to effect of natural convection. The effect of convection on the isothermal lines for $T = 800$ and 1200 is very insignificant.

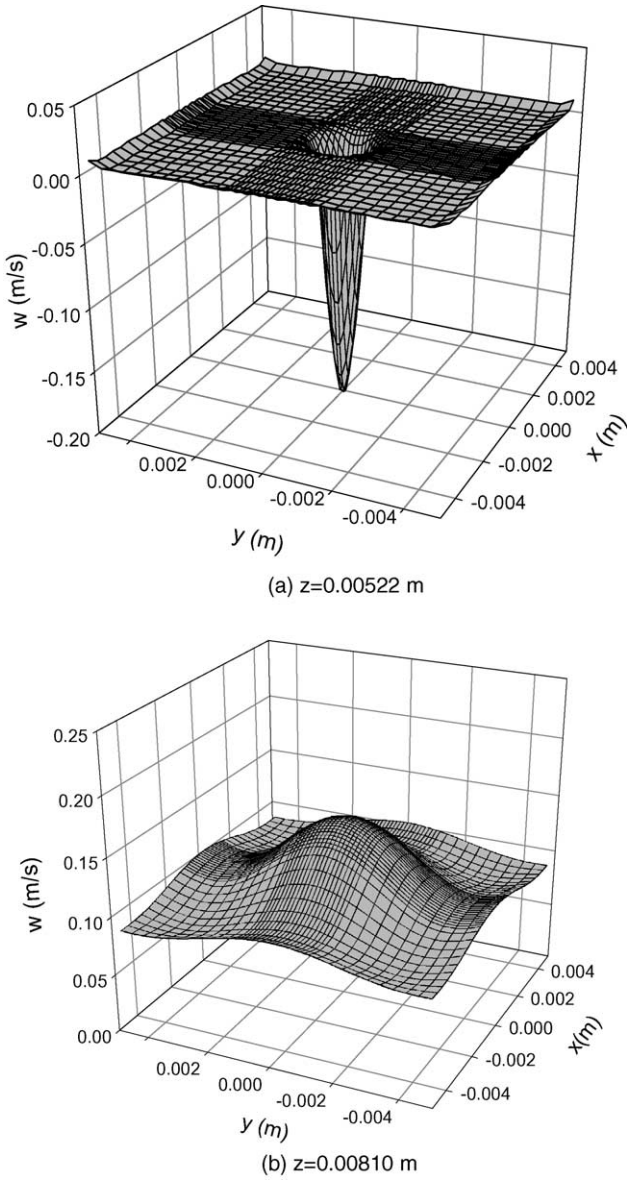

Fig. 3. Velocity component in z direction ($P = 300$ W, $t = 2$ s).

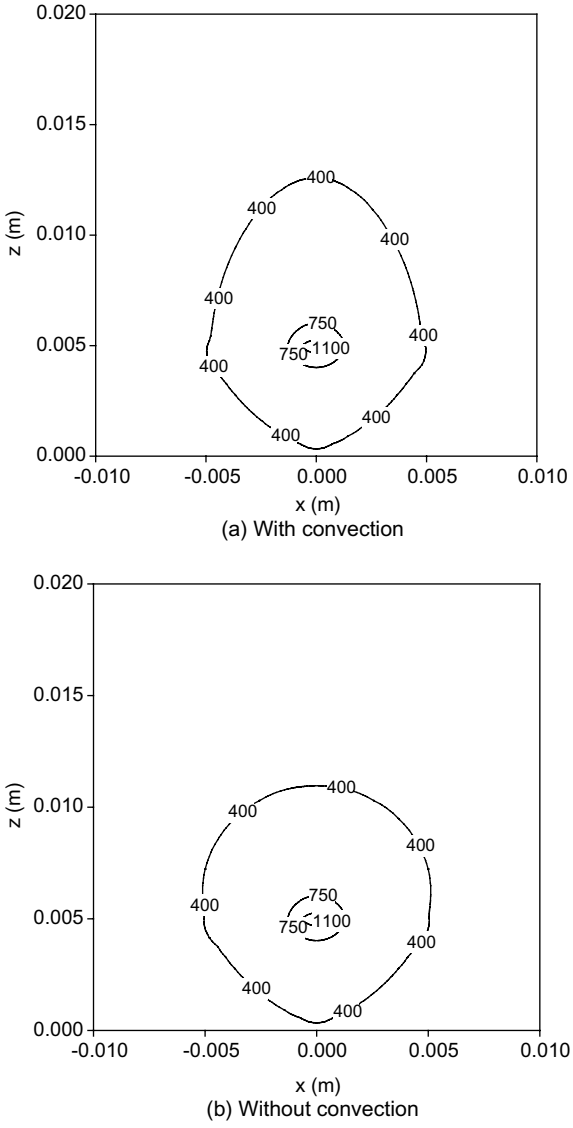

Fig. 4. Temperature contour ($P = 300$ W, $t = 2$ s, $y = 0$).

In order to investigate the effect of laser beam diameter on the LCVD, numerical simulation is performed for $r_0 = 1.414$ mm and the results are plotted in Fig. 8. The laser power and irradiation time is 600 W and 2 s, which resulted in same laser intensity at the center of the laser beam as that of Fig. 2. Although the laser beam intensity at the center of the laser beam is same as that in Fig. 2, volcano-like profile of deposited film is observed because larger power delivered to the substrate surface resulted in higher temperature on the substrate surface (See Fig. 9). Fig. 10 shows a temperature contour at $y = 0$ surface at the end of the process ($t = 2$ s) s for $P = 600$ W, $t = 2$ s, and $r_0 = 1.414$ mm. As can be seen, the isothermal line for $T = 900$ and 1400 K for the cases with and without convection are almost the

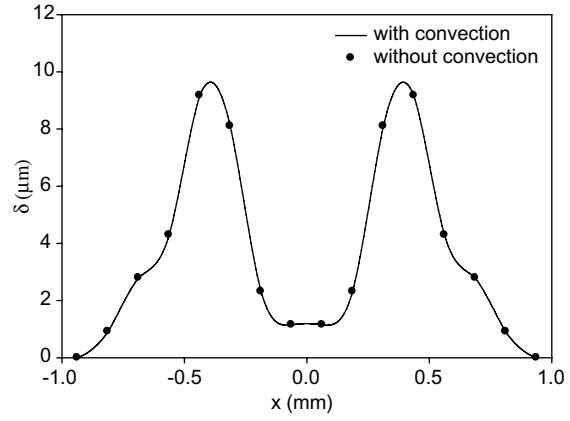

Fig. 5. Effect of convection on the deposited film thickness ($P = 400$ W, $t = 2$ s).

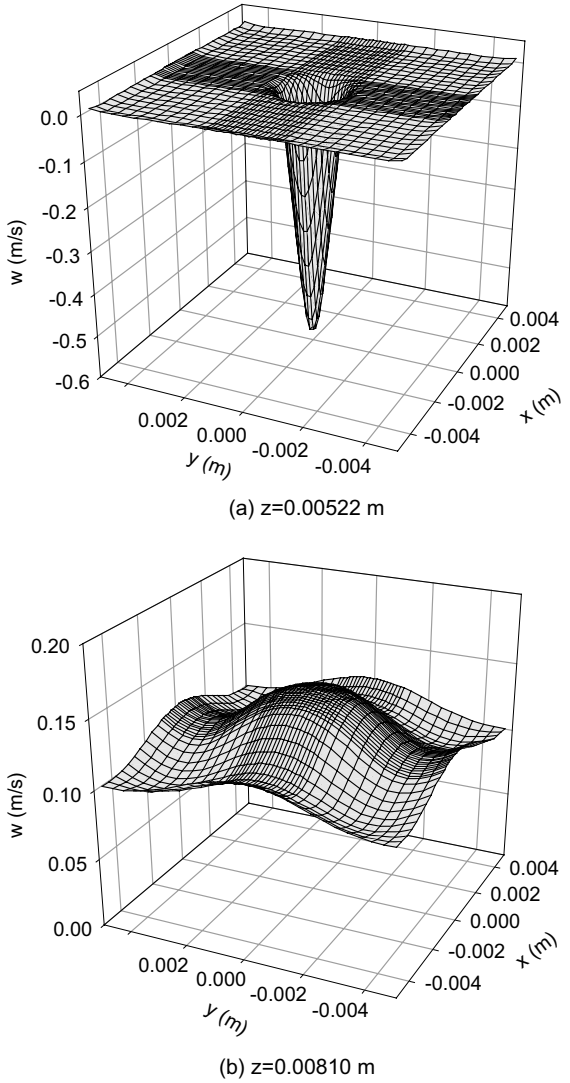

Fig. 6. Velocity component in z direction ($P = 400$ W, $t = 2$ s).

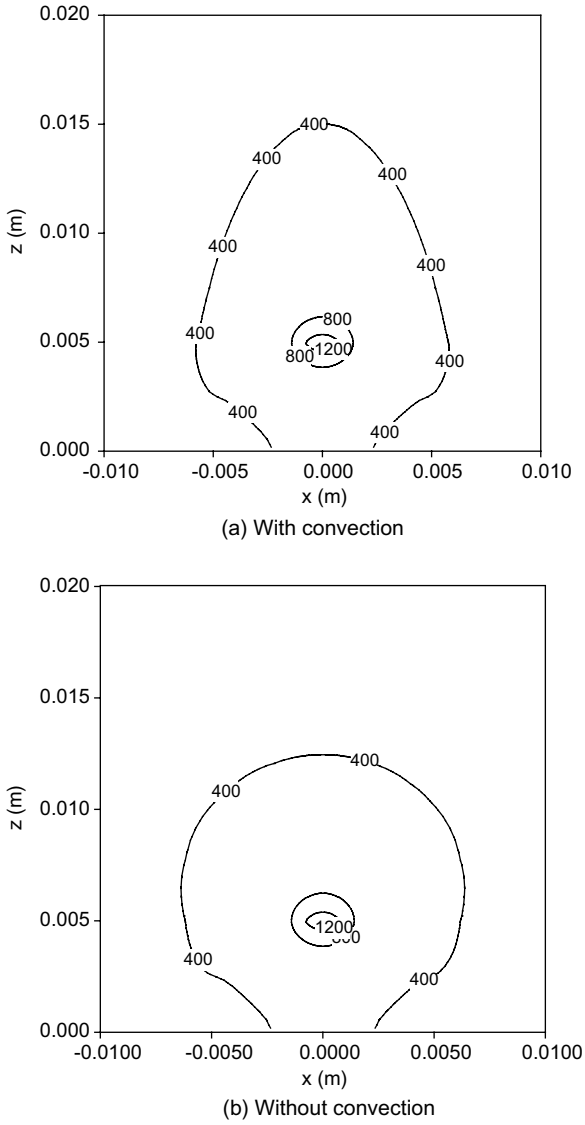

Fig. 7. Temperature contour ($P = 400$ W, $t = 2$ s, $y = 0$).

same, which agree with results in Fig. 9. The isothermal lines for $T = 400$ K for cases with convection is significantly changed due to the effect of natural convection.

Numerical simulation is then performed for the total pressure of 414 Torr and the partial pressure of $TiCl_4$ of 14 Torr, which resulted in doubled initial concentration of $TiCl_4$ as well as hydrogen and nitrogen. Fig. 11 shows predicted deposited TiN film thickness for the case with power of the laser beam and the irradiate time of 300 W and 2 s. The result for case with a total pressure of 207 Torr and same laser power and laser irradiation time is also plotted in Fig. 11 for comparison. It is seen that the deposited TiN film thickness obtained by models with and without convection for doubled total pressure is very close. The difference on film thickness at the center of the laser beam is about 0.06%, which is more than doubled compared to that of total pressure of 207 Torr but it is still very insignificant. Compare the film

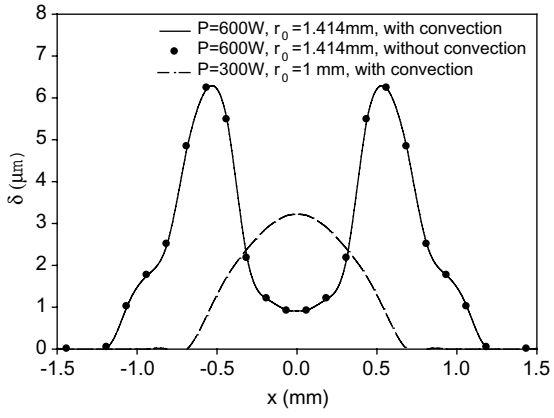

Fig. 8. Effect of laser beam properties on the deposited film thickness.

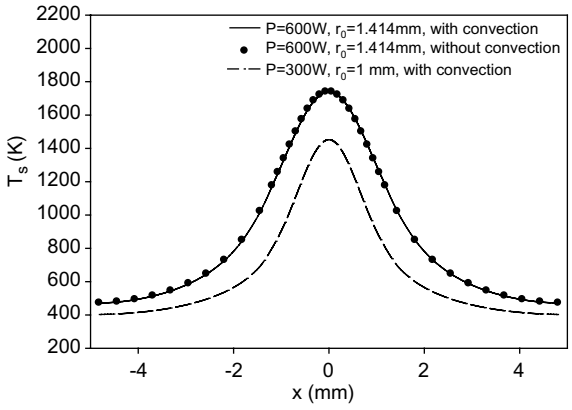

Fig. 9. Profile of the surface temperature of the substrate.

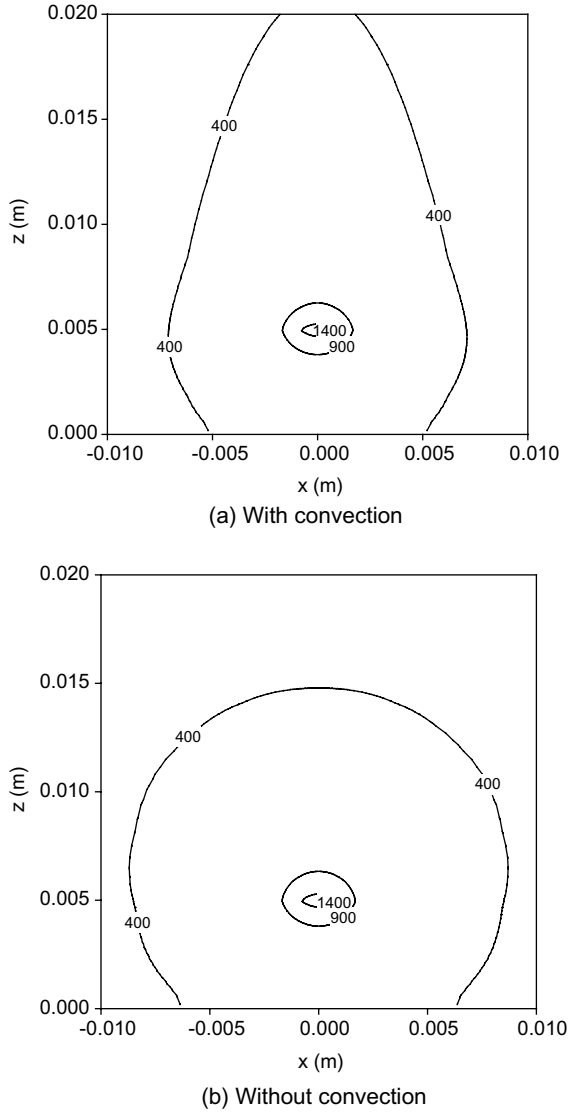

Fig. 10. Temperature contour ($P = 600$ W, $t = 2$ s, $r_0 = 1.414$ mm, $y = 0$).

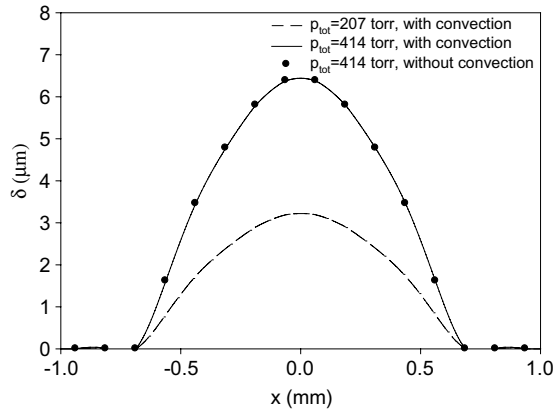

Fig. 11. Effect of initial pressure on the deposited film thickness ($P = 300$ W, $t = 2$ s).

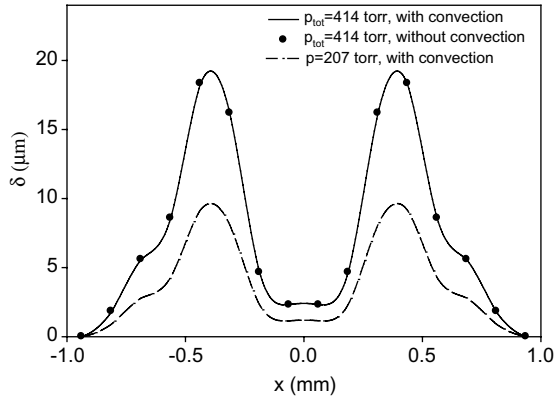

Fig. 12. Effect of initial pressure on the deposited film thickness ($P = 400$ W, $t = 2$ s).

thickness at two different total pressures, the thickness at all location is doubled when the total pressure is doubled. Fig. 12 shows predicted deposited TiN film thickness for the case with the power of the laser beam and the irradiate time of 400 W and 2 s. It can be seen that the effect of convection on the deposited film thickness is very insignificant. The shape of the deposited film with total pressure of 414 Torr is very similar to that with total pressure of 207 Torr, and the thickness at all locations are doubled.

5. Conclusion

Effect of natural convection on the LCVD of TiN film with a stationary laser beam is investigated numerically. The results show that the effect of natural convection on the shape of deposited film is negligible for all cases studied. The velocity components in z direction is negative at the locations near the substrate surface under laser irradiation because chemical reaction takes place on the surface consumed $TiCl_4$. At the locations far

from the substrate surface, the velocity component in z direction near the center of the laser beam is positive due to natural convection driven by the temperature gradient in the gases. Volcano-like profile of the deposited film is obtained when laser beam diameter is decreased and laser power is increased to maintain the same laser beam intensity at the center of the laser beam. The deposited TiN film thickness is doubled when the initial partial pressure of $TiCl_4$, N_2, and H_2 is doubled.

References

Bird, R.B., Stewart, W.E., Lightfoot, E.N., 1960. Transport Phenomena. John Wiley & Sons, New York.

Chase, W.M., 1986. JANAF thermochemical tables, third ed. J. Phys. Chem. Ref. Data, vol. 14 (Suppl. 1).

Conde, O., Kar, A., Mazumder, J., 1992. Laser chemical vapor deposition of TiN Dot: A comparison of theoretical and experimental results. J. Appl. Phys. 72, 754–761.

Conley, J.G., Marcus, H.L., 1997. Rapid prototyping and solid freeform fabrication. ASME J. Manufact. Sci. Eng. 119, 811–816.

Duty, C., Jean, D., Lackey, W.J., 2001. Laser chemical vapour deposition: Materials, modeling, and processing control. Int. Mater. Rev. 46, 271–287.

Jacquot, Y., Zong, G.-S., Marcus, H.L., 1995. Modeling of selective laser deposition for solid freeform fabrication. Proc. Solid Freeform Fabricat. Symp. 1995, 74–82.

Kar, A., Azer, M.N., Mazumder, J., 1991. Three-dimensional transient mass transfer model for laser chemical vapor deposition of titanium on stationary finite slabs. J. Appl. Phys. 69, 757–766.

Kar, A., Mazumder, J., 1989. Three-dimensional transient thermal analysis for laser chemical vapor deposition on uniformly moving finite slabs. J. Appl. Phys. 65, 2923–2934.

Lee, Y.L., Tompkins, J.V., Sanchez, J.M., Marcus, H.L., 1995. Deposition rate of silicon carbide by selected area laser deposition. Proc. Solid Freeform Fabricat. Symp. 1995, 433–439.

Marcus, H.L., Zong, G., Subramanian, P.K., 1993. Residual stresses in laser processed solid freeform fabrication. In: Barrera, E.V., Dutta, I. (Eds.), Residual Stresses in Composites: Measurement, Modeling and Effect on Thermomechanical Properties. TMS.

Maxwell, J., Larsson, K., Boman, M., Hooge, P., Willaims, K., Coane, P., 1998a. Rapid prototyping of functional three-dimensional microsolenoids and electromagnets by high-pressure laser chemical vapor deposition. Proc. Solid Freeform Fabricat. Symp. 1998, 529–536.

Maxwell, J., Shah, J., Webster, T., Mock, J., 1998b. Rapid prototyping of titanium nitride using three-dimensional laser chemical vapor deposition. Proc. Solid Freeform Fabricat. Symp. 1998, 575–580.

Maxwell, J., Boman, M., Williams, K., Larsson, K., Jaikumar, N., Saiprasanna, G., 1999. High-speed laser chemical vapor deposition of. amorphous carbon fibers, stacked conductive coils, and folded helical springs. Part of the SPIE Conference on Micromachining and Microfabrication Process Technology V, SPIE vol. 3874, Santa Clara, CA.

Mazumder, J., Kar, A., 1995. Theory and Application of Laser Chemical Vapor Deposition. Plenum Publishing Co., New York.

Patankar, S.V., 1980. Numerical Heat Transfer and Fluid Flow. Hemisphere, Washington, DC.

Van Doormaal, J.P., Raithby, G.D., 1984. Enhancements of the simple method for predicting incompressible fluid flows. Num. Heat Transfer 7, 147–163.

Williams, K., Maxwell, J., Larsson, K., Boman, M., 1999. Freeform fabrication of functional microsolenoids electromagnets and helical springs using high-pressure laser chemical vapor deposition. Proc. 1999 12th IEEE Int. Conf. Micro Electro Mech. Syst. (MEMS), 232–237.

Yang, M., Tao, W.Q., 1992. Numerical study of natural convection heat transfer in a cylindrical envelop with internal concentric slotted hollow cylinder. Num. Heat Transfer Part A 22, 289–305.

Zhang, Y., 2003a. Quasi-steady state natural convection in laser chemical vapor deposition using a moving laser beam. ASME J. Heat Transfer 125, 429–437.

Zhang, Y., 2003b. A parametric study on shape and cross-sectional area of the thin film produced by laser chemical vapor deposition with a moving laser beam. Proc. 6th JSME–ASME Thermal Eng. Joint Conf., Hawaii Islands, HI, March 16–20, 2003 (CD-ROM).

Zhang, Y., Fgahri, A., 2000. Thermal modeling of selective area laser deposition of titanium nitride on a finite slab with stationary and moving laser beams. Int. J. Heat Mass Transfer 43, 3835–3846.